

Nonlinear Analysis for Hysteretic Behavior of RC Joints Considering Bond-Slip



D. Y. Kim

Abstract This paper presents a numerical model for the analysis of reinforced concrete (RC) joints that explicitly accounts for the bond-slip between the reinforcing bars and the surrounding concrete. A frame element whose displacement fields for the concrete and the reinforcing bars are different from each other to permit slip is introduced. From the fiber section concept, compatibility equations for the concrete, reinforcing bar, and bond are incorporated in the formulation of the element stiffness matrix. For analyses of general loading cases, cyclic stress-strain relations of concrete and reinforcing bar are defined in the material model. For the constitutive model of bond, local bond stress-slip relations for monotonic loads are updated according to the accumulated bond damage at each slip reversal. The numerical applications to the reinforcing bar embedded in the concrete block, RC column anchored in the foundation, and RC beam-column sub-assembly validate the analysis model and show the effect of bond-slip for the assessment of energy dissipation during loading histories.

Keywords Reinforced concrete • Bond-slip • Nonlinear analysis • Frame element

1 Introduction

The fundamental seismic design adopted in the design codes follows the concept of strong column-weak beam so that most of the strain energy is dissipated through the plastic hinge in the beam to prohibit collapse of whole structural system. For a desirable seismic design of the RC joints, one needs to investigate the nonlinear behavior and failure mechanism of the RC joint through analytical modeling as well as an experimental study. Especially, the RC joint shows a complicated structural behavior due to load transfer through bond and shear resistance in the concrete core.

D. Y. Kim (✉)

Civil, Architectural and Environmental Engineering Department, KEPCO E&C,
39660 Gimcheon, Republic of Korea
e-mail: ehdus11@gmail.com

In order to simulate this behavior analytically, a development of numerical model with adequate material constitutive relation is required. To verify the nonlinear behavior of RC joint including the bond-slip mechanism analytically, many numerical studies have been conducted [1, 5, 10].

Since the joint area is a kind of connection part where the sectional properties of connected members change abruptly, it should be modeled with interface elements or bond-slip springs to represent the discontinuous slip at the joint explicitly. However, it is not easy to model the discontinuous behavior in the finite element which is derived based on the continuum mechanics. Most of the related research studies are limited to the development or introduction of simple physical models such as plastic hinges and lumped bond springs [5]. These simple modeling approaches give reliable results to the simple analyses, but it is not suitable to apply these models to general cases having irregular sections with complicated rebar details subject to general multi-directional loading such as earthquake excitations.

In this study, a numerical model is introduced to analyze the RC joints focusing on the bond-slip which significantly affects the hysteretic behavior of the RC joints. A frame element is developed accounting for the effect of bond-slip explicitly by introducing relative displacements between concrete and reinforcing bars. Separate material models for the concrete and reinforcing bar and a bond-slip model for the interaction between two materials are incorporated into the numerical model. In order to validate the developed model and investigate the bond-slip behaviour in the RC member, numerical analyses are conducted for the test specimens.

2 Finite Element Formulation

To develop a frame element considering bond-slip, the beam element [7] which is derived based on the Timoshenko's beam theory is used herein. In this element, the lateral and rotational displacement fields are represented by the nodal lateral and rotational displacements, respectively. Hence, this element could be used effectively to express the compatibility condition of discontinuous slip separating the rotational displacement field of reinforcing bars from that of concrete. The frame element could then be constructed by adding an axial degree of freedom in the beam element [3].

2.1 Displacement Fields

A planar frame element has axial, lateral, and rotational displacement fields. Apart from the displacement field of concrete, the displacement field of reinforcing bars is introduced and connected with a bond spring to account for the slip between two materials (see Fig. 1). Since the reinforcing bars have small sectional area compared to their lengths, the transverse shear deformation of the reinforcing bars could be neglected.

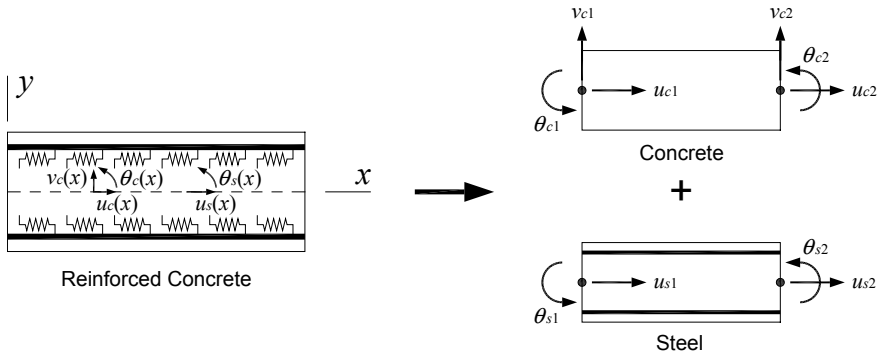


Fig. 1 Displacement fields and DOF of RC frame element considering bond-slip

From this assumption, the displacement field vector of an RC frame element at an arbitrary location has the following form:

$$\mathbf{u}(x) = \{u_c(x) \quad v_c(x) \quad \theta_c(x) \quad u_s(x) \quad \theta_s(x)\}^T \tag{1}$$

where the subscript *c* is for the concrete and the subscript *s* is for the reinforcing bar. As shown on the right side of Fig. 1, this displacement field vector is expressed as the nodal displacement components of concrete and reinforcing bars at each node, i.e.

$$\mathbf{U} = \{u_{c1} \quad v_{c1} \quad \theta_{c1} \quad u_{s1} \quad \theta_{s1} | u_{c2} \quad v_{c2} \quad \theta_{c2} \quad u_{s2} \quad \theta_{s2}\}^T \tag{2}$$

By using shape functions, this nodal displacement vector is expressed as

$$\mathbf{u}(x) = \mathbf{N}(x) \cdot \mathbf{U} \tag{3}$$

where, $\mathbf{N}(x) = \begin{bmatrix} N_1 & 0 & 0 & 0 & 0 & N_2 & 0 & 0 & 0 & 0 \\ 0 & N_1 & 0 & 0 & 0 & 0 & N_2 & 0 & 0 & 0 \\ 0 & 0 & N_1 & 0 & 0 & 0 & 0 & N_2 & 0 & 0 \\ 0 & 0 & 0 & N_1 & 0 & 0 & 0 & 0 & N_2 & 0 \\ 0 & 0 & 0 & 0 & N_1 & 0 & 0 & 0 & 0 & N_2 \end{bmatrix}, N_1 = 1 - x/L,$

$N_2 = x/L$, *L* is the length of an element.

2.2 Compatibility Conditions

Because the reinforcing bars and concrete have different displacement fields, the fiber model in which a section is divided into layers or grids and appropriate material properties are assigned at the corresponding locations is adopted.

Fig. 2 Typical section configuration of RC fiber model

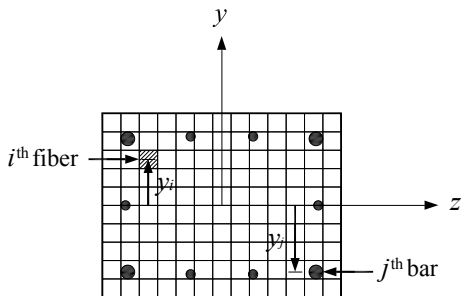


Fig. 3 Compatibility condition for slip

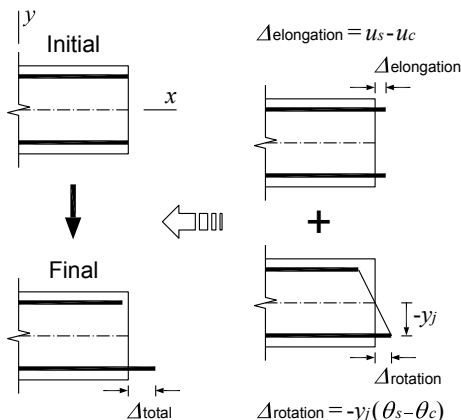


Figure 2 shows a typical section configuration for the fiber model which discretizes the section by grids and calculates the secant modulus, strain, and stress at each grid.

The strain of the concrete at an arbitrary grid is calculated from the axial strain, curvature, and grid location as follows:

$$\epsilon_{ci} = u'_c(x) - y_i \kappa_c(x) \tag{4}$$

in which ϵ_{ci} is the strain of i -th fiber (see Fig. 2) and $\kappa_c \equiv \theta'_c(x)$. Similarly, the strain of the reinforcing bar is calculated from the distance y_j between centroidal axis and center of the reinforcing bar as

$$\epsilon_{sj} = u'_s(x) - y_j \kappa_s(x) \tag{5}$$

in which, $\kappa_s \equiv \theta'_s(x)$. Besides the compatibility conditions for the bending deformation, an additional compatibility condition for the shear deformation is considered. With the assumption that only concrete resists shear deformation, an additional compatibility condition has the following form [3, 7]:

$$\gamma = v'_c(x) - \theta_c(x) \tag{6}$$

in which $v'_c(x)$ is the derivative of concrete lateral displacement with respect to x .

For the compatibility condition of the slip, the differences in elongation and rotation between two materials are considered as schematically depicted in Fig. 3. For clarity, the displacements of concrete are not shown. The final slip at any rebar location is determined from the combination of axial and rotational displacement differences as

$$\Delta_j = u_s(x) - u_c(x) + (\theta_s(x) - \theta_c(x)) \cdot (-y_j) \tag{7}$$

2.3 Sectional Stiffness

The sectional stiffness of the RC frame element is calculated from the construction of sectional stiffness of each material, such as the axial rigidity and moment of inertia, and bond stiffness between the two materials. The axial and rotational components in the sectional stiffness matrix are calculated from the material and sectional information of each grid and reinforcing bar as given by

$$\mathbf{D}_c = \sum_{i=1}^m \begin{bmatrix} E_{ci}A_{ci} & 0 \\ 0 & y_i^2 E_{ci}A_{ci} \end{bmatrix}, \mathbf{D}_s = \sum_{j=1}^n \begin{bmatrix} E_{sj}A_{sj} & 0 \\ 0 & y_j^2 E_{sj}A_{sj} \end{bmatrix} \tag{8a}$$

and the sectional shear stiffness is calculated from

$$D_\gamma = GA^* \tag{8b}$$

in which m is the total number of grids in the section, E_{ci} the Young's modulus, A_{ci} the area of i th grid, n the number of reinforcing bars in the section, and E_{sj} and A_{sj} are the Young's modulus and area of j th reinforcing bar, respectively. For the shear, G is sectional shear modulus and A^* is effective area [3]. Since this study is focused on the combination of bending and axial behavior, the shear behavior is assumed to be elastic.

Generally, the amount of slip in each reinforcing bar is different from each other. Hence, the stiffness matrix for the bond could be constructed by extending the bond property of each reinforcing bar to the whole of reinforcing bars as follows:

$$\mathbf{D}_\Delta = \begin{bmatrix} E_{b1}p_1 & \cdots & 0 \\ \vdots & \ddots & \vdots \\ 0 & \cdots & E_{bn}p_n \end{bmatrix}_{n \times n} \quad (9)$$

where E_{bj} is the Young's modulus obtained from hysteresis curve of bond-slip material model of j th reinforcing bar and p_j is the perimeter of j th reinforcing bar.

The element stiffness matrix and internal force vector of the frame element are then obtained from applying the principle of virtual work.

3 Material Model

3.1 Concrete and Reinforcing Bar

Since the bond behavior is considered explicitly in the finite element, tension-softening effect by the fracture energy of concrete itself is only incorporated in the tensile stress-strain curve ignoring tension-stiffening effect [2]. The confinement effect provided by transverse reinforcement such as stirrups is considered in the fiber model by introducing different compressive stress-strain curves inside and outside the stirrup in the fiber section. Based on the monotonic stress-strain relations, a generalized cyclic stress-strain relation is constructed with unloading and reloading branches [8]. A linear elastic, linear strain hardening model is adopted for the monotonic curve of reinforcing steel. Among a number of models developed to describe the cyclic stress-strain curve of reinforcing steel, the model introduced in CEB [2] is adopted herein.

3.2 Bond-Slip Model

The bond-slip relationships representing the resistance against interfacial slip between concrete and rib of a deformed bar are proposed by many researchers through pull-out and splitting tests of reinforcing bar embedded in concrete [4–6]. The bond stress-slip relationships for both of pull-out and splitting failures are proposed by experimental work [6] and are adopted in this study (see Fig. 4). Some representative points are calculated from compressive strength of concrete, diameter of reinforcing bar, cover depth, and reinforcement ratio of stirrup [6].

Fig. 4 Local bond stress-slip relation

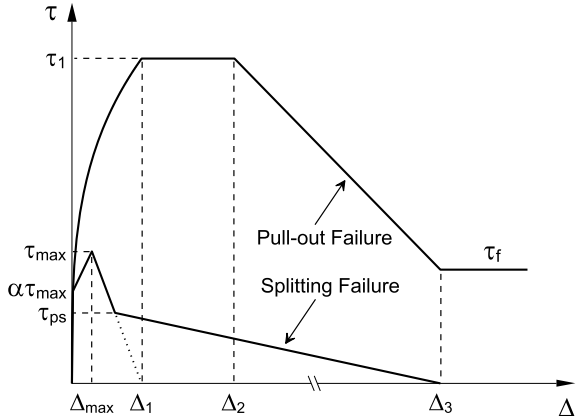
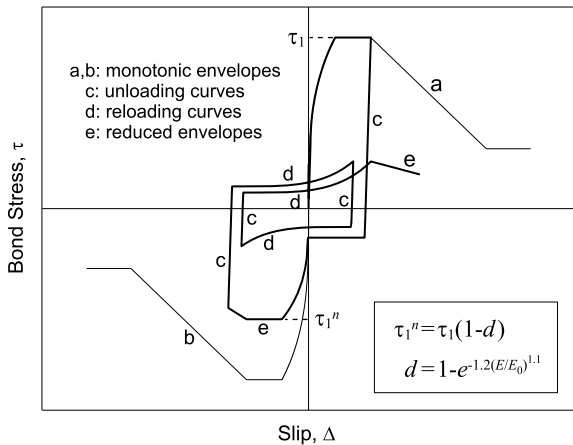


Fig. 5 Hysteretic bond stress-slip curve



For the cyclic bond-stress slip relationship, very limited experimental researches for model development are performed [5]. A hysteretic bond stress-slip model is proposed by Eligehausen et al. [4] through pull-out tests of reinforcing bar embedded in concrete block and is adopted in this study. In this model, a damage parameter, d , which is defined by the accumulated area of hysteretic bond stress-slip curve during slip history and the area of monotonic curve, is introduced (see Fig. 5).

4 Numerical Analysis

4.1 Embedded Reinforcing Bar

For a fundamental study of bond behavior in the RC member and verification of the bond-slip model, a numerical analysis is conducted with the test specimen of reinforcing bar embedded in the concrete block [12]. The specimen is subjected to cyclic push-pull displacements at the ends of the reinforcing bar. The embedment length of test specimen is 25 times the diameter of reinforcing bar and other material properties of the reinforcing bar are summarized in Table 1.

Table 1 Material properties of reinforcing bar

Anchorage length (mm)	Reinforcing bar		
	d_b (mm)	f_y (MPa)	E_o (MPa)
635	25.4	483	29,000

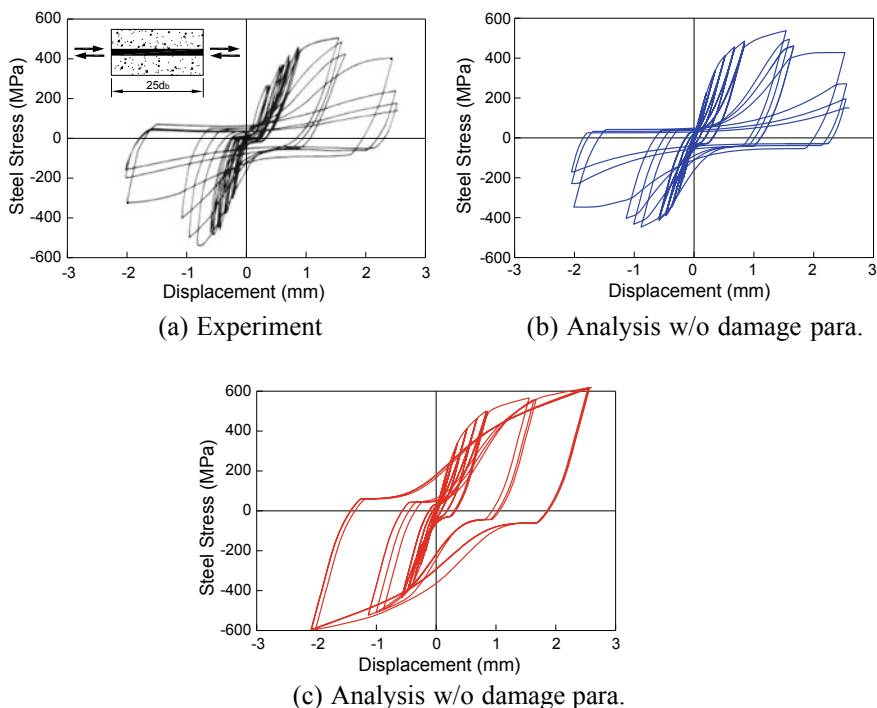


Fig. 6 Cyclic stress-displacement relation of reinforcing bar embedded in concrete

In this example, axial degrees of freedom of reinforcing bar and concrete in the frame element are used only. Since this test is performed with fully confined condition, the displacement of concrete could be ignored and the pull-out failure could be assumed in the material model. Evenly spaced twenty-five elements are used to model the specimen. Figure 6(a) shows the experimental result of stress-displacement history of reinforcing bar at the rightmost side of the specimen. To see the analytical effect of bond damage accumulated during slip histories, analysis results with and without consideration of damage parameter, d in the bond-slip hysteresis curve are shown in Figs. 6(b) and (c), respectively.

If the reinforcing bar experiences small displacement with low level of slip reversal before yielding, stresses are transferred well along the length of the specimen. However, as the bond damage increases after yielding of reinforcing bar at both ends, a bond failure occurs before stresses are developed inside the block, resulting in abrupt decrease of resisting force. The analysis results with consideration of damage parameter shows a good agreement with experimental results. An overestimation of the energy absorption is observed in the analysis results without consideration of damage parameter.

4.2 RC Column

To obtain bond-slip effect in the behavior of simple structural member, an axially and laterally loaded RC column specimen tested by Low and Moehle [9] is analyzed. Figure 7 shows the configuration of the test specimen and its cross section with reinforcing bar layout. The compressive strength of concrete is 36.5 MPa and three different types reinforcing bars are used (see Fig. 7). The finite element discretization used are shown in Fig. 8. The column and anchorage parts are modeled with 20 and 14 evenly spaced elements, respectively. The cross-section is idealized with fiber model with confined and unconfined stress-strain curves of concrete. Compared to the column part, relatively large axial and rotational stiffness is applied to the concrete of the anchorage part.

Fig. 7 Geometry and section configuration of RC column specimen

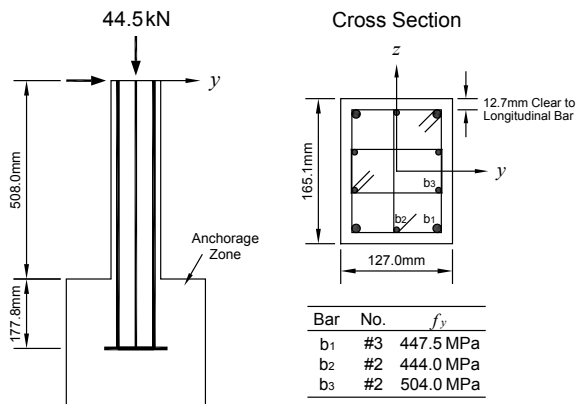
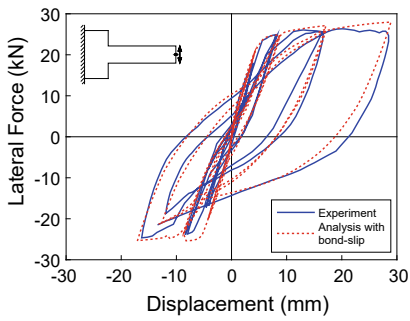
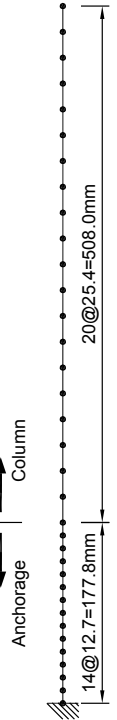
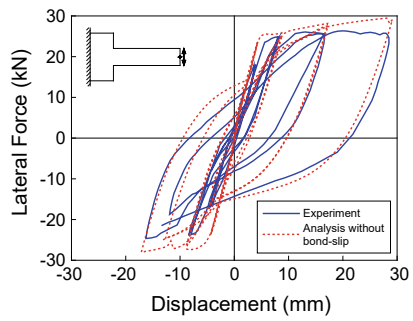


Fig. 8 Finite element idealization of RC column specimen



(a) With bond-slip effect



(b) Without bond-slip effect

Fig. 9 Force-displacement relations of RC column specimen

As shown in Fig. 7, the column specimen is subjected to the combined action of axial load (44.5 kN which causes stress equivalent to 5% of f'_c) and horizontal displacements histories to the y direction. The same conditions are applied to the numerical analysis and force-displacement relations at the top of column are compared in Fig. 9.

From the analysis results, it is shown that the effect of bond-slip on the peak strength after yielding is not so much. This is due to the fact that the peak strength is maintained regardless of increase of displacement due to the embedment length and modeling of hooked anchorage. Hence, as shown in the experiment, bond failure does not occur in the analysis. However, the simulated unloading and reloading curves considering bond-slip show better agreement with the experimental results and evaluate energy dissipation capacity exactly.

4.3 Beam-Column

To simulate the RC joint behavior under lateral loading history and to see the bond-slip effect of the developed frame element, one of the beam-column specimens tested by Soleimani et al. [11] is analyzed. This specimen governs bond failure of the reinforcing bar rather than joint shear failure. The geometry and cross-section dimensions of the test specimen is presented in Fig. 10. The material properties of concrete and reinforcing bars used in the analysis are the same as those of the test specimen and summarized in Table 2.

Table 2 Material properties of beam-column specimen

Concrete f_c' (MPa)	Reinforcing bar			
	Bar no.	d_b (mm)	f_y (MPa)	E_o (MPa)
29.9	#2	6.35	445	29,000
	#5	15.9	492	29,000
	#6	19.1	490	29,000

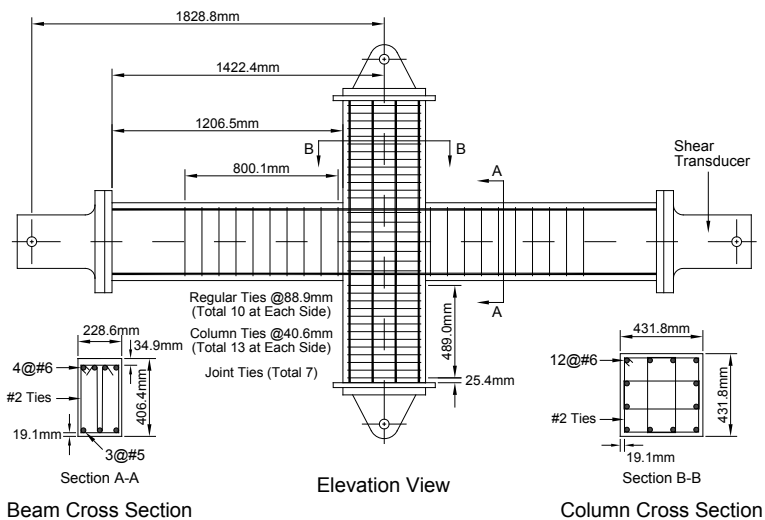


Fig. 10 Configuration of beam-column specimen

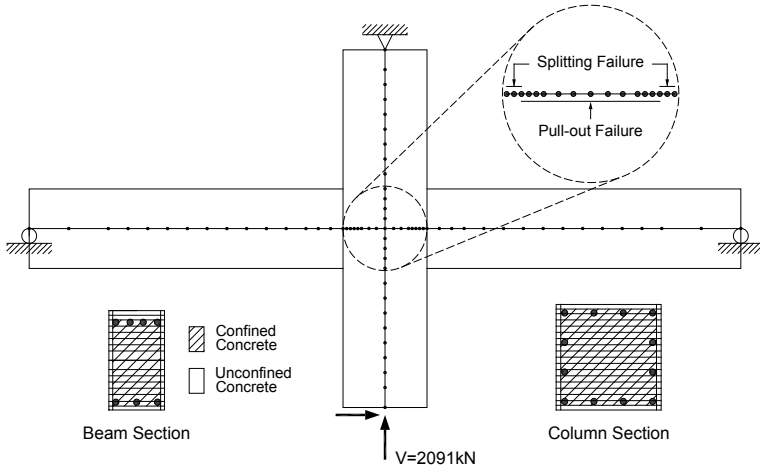


Fig. 11 FE idealization of beam-column

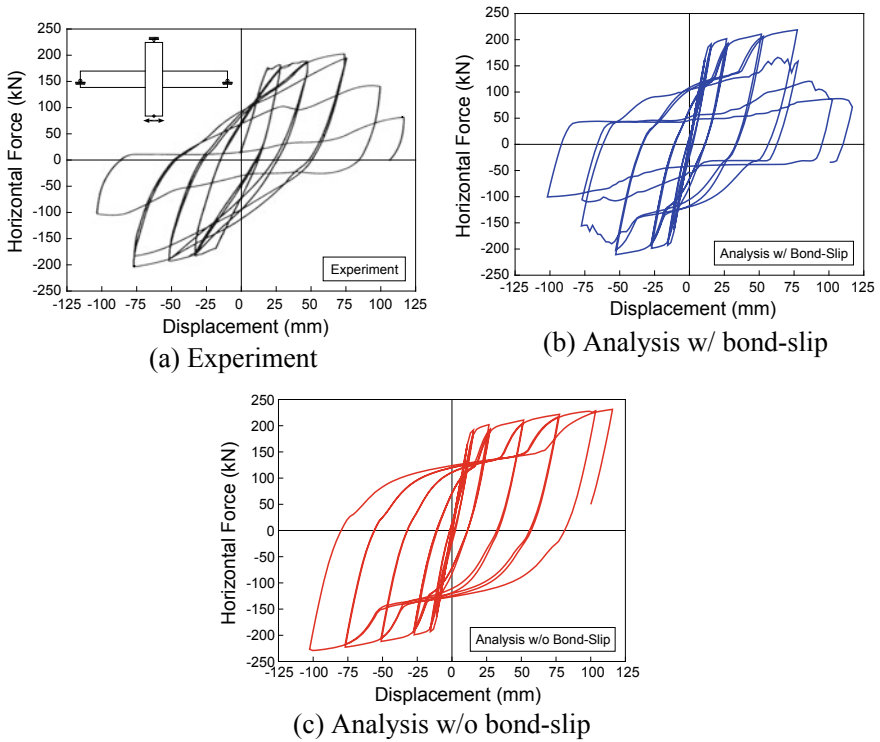


Fig. 12 Hysteretic force-displacement relation beam-column

As shown in Fig. 11, a dense finite element mesh is used to model the joint location. To ignore the deformation of concrete in the beam elements inside the joint, relatively large axial and rotational stiffnesses are assumed. Because the unconfined part which is outside the stirrup in the column is governed by a splitting failure, different bond-stress slip relations (see Fig. 4) are assigned in the inside and outside the stirrup (see the dotted enlarged part in Fig. 11). A constant axial load of 2,091 kN is applied first at the bottom of column, and then the lateral displacement history is applied at the same location based on the concept of ductility. In order to investigate the contribution of bond-slip effect to the nonlinear structural response, the hysteretic force-displacement relationships obtained from the analysis with and without consideration of bond-slip are compared with those from the experiment in Fig. 12.

As displacement histories are accumulated, slip of the main reinforcing bar at the joint increases causing a bond failure when the ductility ratio is over 6. This leads to an abrupt reduction of energy absorption. Figure 12 shows that the analysis with consideration of bond-slip predicts well the bond failure and reduction of energy dissipation capacity.

5 Conclusions

A numerical model and its application to the hysteretic analyses of RC joints are introduced in this study. A frame element which has independent displacement fields for the concrete and reinforcing bars is developed to account explicitly for the slip between the two materials. Based on the different displacement fields of the two materials, fiber section concept, and compatibility conditions for strain and slip with material models, a finite element is constructed.

The developed model is validated through comparison of the obtained numerical results with experimental data from embedded reinforcing bar, RC column, and beam-column joint. The hysteretic behaviors are well predicted with consideration of bond-slip simulating appropriately the accumulated bond damage and energy dissipation during loading histories.

Acknowledgements This work was supported by the Basic Science Research Program received through the National Research Foundation of Korea (NRF) funded by the Ministry of Science and ICT (NRF-2017M2A8A4014828). The information presented in this paper represents the opinions and views of the author and does not necessarily reflect the views of the sponsoring agencies.

References

1. Ayoub A (2006) Nonlinear analysis of reinforced concrete beam-columns with bond-slip. *J Eng Mech ASCE* 132(11):1177–1186
2. CEB (1996) RC elements under cyclic loading: state of the art report, Thomas Telford Services Ltd., London
3. Cook RD, Malkus DS, Plesha ME, Witt RJ (2002) Concepts and applications of finite element analysis. Wiley, New York
4. Eligehausen R, Popov EP, Bertero VV (1983) Local bond stress-slip relationships of deformed bars under generalized excitations. Report No. UCB/EERC-83/23, University of California, Berkeley, California
5. fib (2014) Bond and anchorage of embedded reinforcement: Background to the fib Model Code for Concrete Structures 2010, Bulletin No. 72, Fédération internationale du béton, Swiss
6. Harajli MH, Hamad BS, Rteil AA (2004) Effect of confinement on bond strength between steel bars and concrete. *ACI Struct J* 101(5):595–603
7. Hughes TJR, Taylor RL, Kanoknukulchai S (1977) A simple and efficient finite element for plate bending. *Int J Numer Meth Eng* 11(10):1529–1543
8. Kim DY (2004) Cracking and hysteretic behavior of reinforced concrete shear walls. Ph.D. Dissertation, Korea Advanced Institute of Science and Technology
9. Low SS, Moehle JP (1987) Experimental study of reinforced concrete columns subjected to multi-axial cyclic loading. Report No. UCB/EERC-87/14, University of California, Berkeley, California
10. Maekawa K, Pimanmas A, Okamura H (2003) Nonlinear mechanics of reinforced concrete. Spon Press, London
11. Soleimani D, Popov EP, Bertero VV (1979) Hysteretic behavior of reinforced concrete beam-column subassemblages. *ACI J Proc* 76(11):1179–1195
12. Viwathanatepa S, Popov EP, Bertero VV (1979) Effects of generalized loadings on bond of reinforcing bars embedded in confined concrete blocks. Report No. UCB/EERC-79/22, University of California, Berkeley, California